TESTING Nb3Sn COATING USING μSR

R.E. Laxdal, T. Buck, TRIUMF, Vancouver, Canada
M. Liepe, S. Posen*, Cornell, Ithaca, USA
R. Kiefl, S. Gheidi, UBC, Vancouver, Canada

Abstract

The SRF group at TRIUMF has tested samples relevant for SRF application since 2010 using the TRIUMF μSR facility. In this study collaborators at Cornell coat a Nb coin and a Nb ellipsoid sample with Nb3Sn for characterization using μSR at TRIUMF. Field of first flux entry measurements are performed at M20 on both samples. Measurements include the vortex nucleation field $H_{nucleate}$ and T_c of both Nb3Sn and Nb. Interestingly the Nb3Sn increases the vortex nucleation field at 2K over standard Nb samples.

INTRODUCTION

μSR (muon spin rotation) is a powerful condensed matter technique to characterize superconductors in terms of their magnetic-phase diagram. Since 2010 the SRF group at TRIUMF has been using the μSR technique to characterize materials and processing techniques typical for the SRF community using the TRIUMF surface muon beam [1][2]. Typical samples have been prepared from RRR Nb either as coins or in a machined ellipsoid geometry. In this paper we present results on measurements of a Nb coin and ellipsoid each coated with a 2 μm layer of Nb3Sn.

The performance of niobium as an SRF material is reaching critical limits in terms of surface resistance and peak surface field. Alternative superconductors to niobium are being developed to offer a way to push performance beyond Nb. One very promising material is Nb3Sn, a Type-II superconductor with a relatively high Kappa (~40) as opposed to 1.4 for Nb. Nb3Sn has a relatively high critical temperature, 18K, double that of Nb which allows for example to operate 1.3GHz cavities at 4.2K with the same losses as for Nb at 2K. Although H_{c1} for Nb3Sn is relatively low, 38mT, as opposed to 170mT for Nb, Nb3Sn has a high superheating field, 400mT, compared to 220mT for Nb and an extended mixed phase with an H_{c2} of ~30T.

A Nb3Sn SRF program began at Cornell University in 2009. The program has achieved some significant milestones with a 1.3GHz single cell cavity: (1) reproducible high Q0 on the order of 10^{10} at 4.2 K, (2) reproducible sustaining of this high Q0 to useful gradients ~14 MV/m, and (3) reproducible H_{pk} significantly higher than H_{c1} with no strong degradation, showing that it is not a limit [3].

A comparison of the main superconducting properties of Nb and Nb3Sn (close to stoichiometric) is presented in Table 1 [4] at $T = 0$. The goal of this experiment is to characterize the performance of Nb3Sn in terms of its ability to repel magnetic field as a function of temperature.

Table 1: Superconducting Properties of Nb and Nb3Sn

Property	Nb	Nb3Sn
Tc [K]	9.2	18
$\mu_0 H_{c1}$ [T]	0.17	0.038
$\mu_0 H_c$ [T]	0.2	0.52
$\mu_0 H_{c2}$ [T]	0.4	30
$\mu_0 H_{sh}$ [T]*	0.24	0.43
$\xi GL(0)$ [nm]	29	3.3
$\lambda eff(0)$ [nm]	41	135
$\kappa(0)$	1.4	41
$\Delta(0)$ [meV]	1.4	3.4

*All values quoted from [4] except H_{sh} which is computed from [5]

$$H_{sh} = H_c \cdot \left(\frac{\sqrt{20}}{6} + \frac{0.55}{\sqrt{\kappa}} \right) \quad (1)$$

EXPERIMENTAL METHOD

μSR Technique

In a μSR experiment, 100% spin polarized muons are implanted one at a time into the sample, stop in interstitial sites and precess with characteristic Larmor frequencies determined by the local magnetic field. The geometry of the TF measurement is illustrated in Fig. 1. The muons travel down the beam line and pass through an initial muon counter that starts an electronic clock. The muons then pass through a silver mask with an 8mm diameter hole in the centre used to restrict the measured muons to the centre of the sample. The muons will decay with a
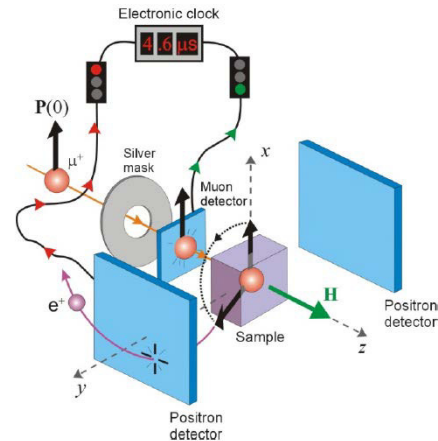

Figure 1: TF-μSR setup with the initial muon spin polarization perpendicular to the magnetic field. The silver mask in front of the sample restricts the muon implantation to the central region of the sample.

*now at FNAL

half-life of 2.2μs, and emit positrons which have a propensity to emerge along the direction of the muon spin. Two positron detectors (symmetrical placed around the sample) detect the positron signal and stop the clock. The time evolution of muon spin polarization $P_z(t)$ is sampled by calculating the asymmetry of the signal in the two detectors. The asymmetry signal gives information concerning the volume fraction of the host material sampled by the muon that contains magnetic field. This signal can be used to characterize the superconducting state, particularly the transition from Meissner state to mixed state. When completely in the Meissner state there is no field in the sample and the asymmetry is maximized. As the field increases flux will eventually enter the superconductor as it enters the mixed state and the asymmetry signal will be reduced. The sample geometry is a key parameter as demagnetizing effects are important in determining the field of first flux entry.

Expected Meissner Screening

Nb3Sn is deposited on a RRR Nb substrate to a depth of about 1-2micron. The muons are deposited at ~150 μm into the Nb bulk. When the maximum field at the surface ($H_{surface}$) of the superconductor exceeds H_{c1} of the material (or up to H_{sh} depending on the geometry) the material will enter the mixed phase. Depending on the temperature and applied field Meissner screening could come either from the Nb3Sn coating or the Nb bulk. For the following we assume that surface imperfections or geometry effects mean that H_{c1} is the limitation for vortex penetration. We will revisit this assumption in the discussion. At 2K both the Nb and Nb3Sn are superconducting and surface currents will be set up in the Nb3Sn layer until $H_{c1}(T)$ [Nb3Sn] and in the Nb London layer from $H_{c1}(T)$ [Nb3Sn] $< H_{surface} < H_{c1}(T)$[Nb] with the Nb3Sn coating in the vortex state. For higher temperatures the critical fields are reduced as per the relation

$$H_{c1}(T) = H_{c1}(0) \cdot \left(1 - \left(T/T_c\right)^2\right) \qquad (2)$$

For temperatures in excess of T_c[Nb]=9.2K the Nb is normal and non-magnetic and any screening will come only from the Nb3Sn. A summary of the combined H_{c1} for the Nb3Sn coating on Nb bulk samples is shown in Fig. 2.
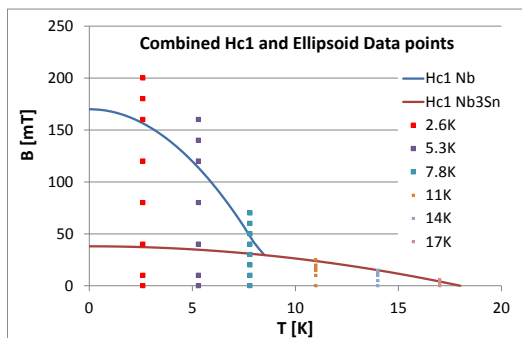

Figure 2: Combined H_{c1} for the Nb3Sn on Nb samples and data points for the ellipsoid characterization.

Test Geometry

In this study two sample types, coin and ellipsoid, and three different combinations of sample and field/muon geometry are employed as shown in Fig. 3a,b,c. The coin can be placed in transverse fields with the muons aligned with the field and applied to the face or parallel with the field with the muon path perpendicular to the field orientation and again applied to the coin centre. The ellipsoids are aligned with the applied field and the muons are implanted at the pole. Most straightforward are geometries (a) and (c) where the muon and magnetic field are aligned and the muon is not deflected by the Lorentz force. A new beamline has recently been added to allow for the first time testing samples in strong magnetic fields transverse to the muon path [6]. In all cases an 8mm diameter mask is used to locate the muons on the sample.
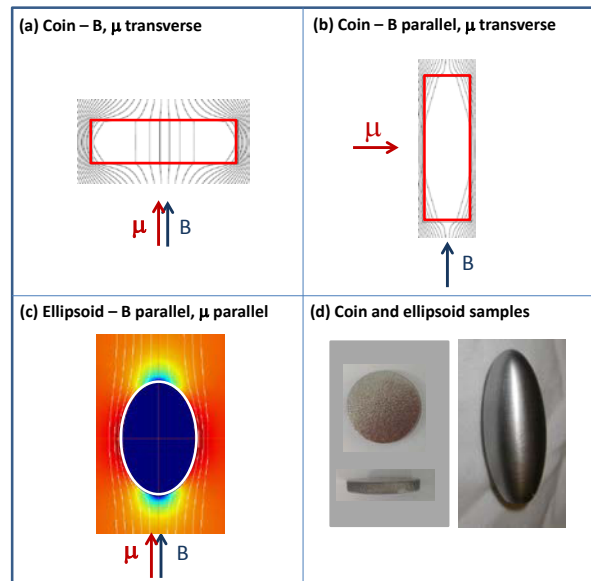

Figure 3: (a,b,c) Three arrangements of sample (coin and ellipsoid), muon and field direction for the Nb3Sn sample characterization studies with μSR. The actual samples are shown in (d).

Data Acquisition

Fig. 2 also indicates the data points taken to characterize the Nb3Sn coated ellipsoid. Each of the 38 points corresponds to a ~30 minute run to collect asymmetry statistics. Approximately four 12 hour shifts are required for the characterization. The sample is first cooled to the desired temperature in zero field to eliminate trapped flux. Then the field is raised sequentially while the temperature is regulated. When one temperature set is completed the sample is warmed to 25K, the field is zeroed and the sample is cooled again to the next temperature. The data taking proceeds through all the temperature steps in this way.

The coin sample is tested at two temperatures, 2.5K and 11K, for both the parallel and transverse orientations. In parallel geometries the muons are first pre-steered off axis before being bent back to the sample from the dipole providing the field on the sample.

SAMPLES

Description

Coin samples are cut from Nb sheet while ellipsoids are machined from bulk Nb. The material in both cases is RRR fine grain Nb. One coin sample and one ellipsoid were coated with a 2 μm thick layer of Nb3Sn at Cornell. The coating procedure is the same as successfully used on the RF cavities [7]. Coating lasts 3 hours, with the cavity at 1100C and the tin source at 1200C. The coins are 3mm thick and 20mm in diameter. The prolate ellipsoids are 9mm in radius on the minor axis with a 22.9 mm semi-major axis. A threaded hole is drilled in one end of the ellipsoid for mounting the sample during coating and during the test. The other pole is the one facing the muon beam for implantation. The samples are shown in Fig. 3d.

Geometry Considerations

Ellipsoid samples: The Meissner state is supported by screening currents that augment the field at the equator and reduce the field at the poles (Fig. 3c). When the flux at the equator reaches $H_{nucleate}$, fluxoids will nucleate at the equator and redistribute uniformly inside the superconductor due to vortex repulsion for a pin free sample. Pin-free ellipsoidal bulk samples produce a uniform vortex flux density in the mixed state since the inward directed driving force on the vortex ends by the surface screening currents is compensated by the vortex line length that increases for fluxoids closer to the ellipsoid axis. The magnetic field will be enhanced at the equator by a factor related to the demagnetizing factor N by $H_{equator}=H_{applied}/(1-N)$ where $H_{applied}$ is the applied field. In our geometry the ellipsoid demagnetizing factor is $N = 0.13$ with $H_{applied}|_{entry}=0.87H_{nucleate}$. In the case of samples with pinning the redistribution will be affected as the pinning centers will add a frictional component to the redistribution such that fluxoids will tend to preferentially populate nearer the equator and will only gradually reach the poles as the field increases beyond $H_{applied}|_{entry}$.

For ellipsoidal shells (Nb3Sn coating) the situation is similar to bulk ellipsoids in terms of magnetization except that after nucleation the fluxoids will snap to the center since the flux line length in the superconducting shell is actually less near the ellipsoid axis so that pinning would be less dominant in resisting nucleated flux to move to the poles.

Coin samples: For field applied perpendicular to the face the magnetic field will be enhanced at the edges of the coin by a factor related to the demagnetizing factor *N*. For Type II superconductors when the applied field is such that the enhanced field at the edges reaches H_{c1} the field will break into the edge such that the local field is reduced due to the rounding of the flux line. As the field increases the flux lines will cut further across the corner and eventually join at the centre of the sample edge. This corresponds to $H_{nucleate}$ and is higher than H_{c1} due to the so called edge boundary [8]. The flux line is driven inwards due to interaction with the surface currents so that in a pin-free sample the flux will move to the centre (Fig. 4)

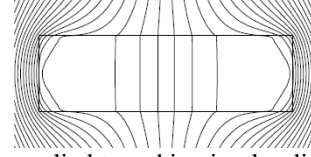since this represents the lowest energy position (minimum line tension).

Figure 4: Flux applied to a thin circular disk transverse to an applied field where $H_{applied}> H_{applied}|_{entry}$.

As the flux increases and vortices multiply the vortex currents will repel so that the flux lines will redistribute and fill from the centre to the outside edge. In our case for the standard coin geometry the demagnetizing factor is $N=0.77$ meaning that at $H_{applied}|_{edge}=0.23H_{c1}$ flux breaks in at the edge while at $H_{applied}|_{entry}=0.31H_{c1}$ flux breaks to the centre. For a sample with pinning the pinning centres act as additional barriers adding 'resistance' to the mobility of vortices moving from the edges to the centre and increasing the required applied field for flux entry compared to the pin free case.

Considering a superconducting shell the geometric boundary is eliminated since as soon as flux breaks into the corners the fluxoid will snap to the centre for a pin free shell. In this case $H_{applied}|_{entry}=0.23H_{c1}$.

In a parallel geometry the bulk coin has an estimated demagnetization factor of $N=0.22$ with break in field enhanced by edge boundary of $H_{applied}|_{entry}=0.91*H_{c1}$. In this case flux could still be pinned at the corners before joining at the center (pinning enhanced edge boundary) but much less so than in the transverse geometry. For a superconducting shell in parallel geometry we expect $H_{applied}|_{entry}=0.78*H_{c1}$ similar to the transverse geometry. Results are summarized in Table 2.

Table 2: Demagnetization Factors and Applied Fields, $H_{apply}|_{entry}$, for Entry for Pin Free Samples

Sample	SC type	N	$H_{apply}|_{entry} /H_{c1}$
Transverse coin	bulk	0.77	0.31
Parallel Coin	bulk	0.2	0.91
Ellipsoid	bulk	0.13	0.87
Transverse coin	shell	0.77	0.23
Parallel Coin	shell	0.22	0.78
Ellipsoid	shell	0.13	0.87

RESULTS

Ellipsoid

A summary plot of all calculated normalized asymmetries for all ellipsoid runs is shown in Fig. 5. A normalized asymmetry of unity means that there is no magnetic field detected in the sample volume probed by the muon. The data shows clearly the penetration of flux as the Meissner state breaks down. As the temperature is increased the amplitude of the penetrating field is reduced as expected. A detail of the data for T>9K is shown in Fig. 6.
The normalized asymmetry plots are analysed to extract the applied field required for flux penetration. The resulting data is show in Table 3. The nucleation field is
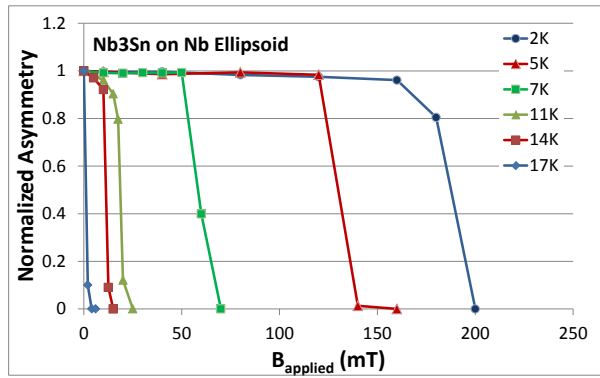
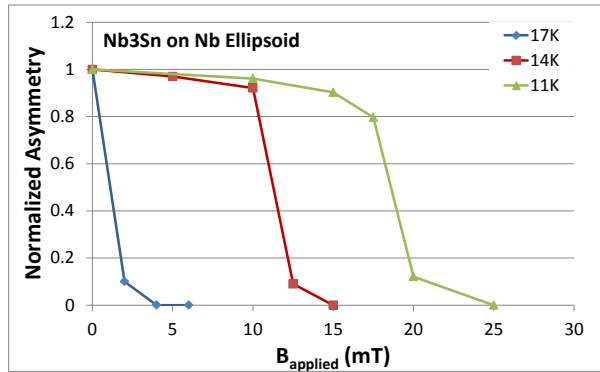Figure 5: Summary of normalized asymmetry for all runs for the ellipsoid geometry.

Figure 6: Detail of the normalized asymmetry for the runs with the ellipsoid geometry for data where T>9K.

computed by employing the field enhancement factor from the demagnetization as noted in Table 2.

Equation 2 yields the linear equation

$$\frac{H_{nuc}(T)}{H_{nuc}(0)} = 1 - \left(\frac{T}{T_c}\right)^2 \tag{3}$$

The data from Table 3 is grouped into Nb data for T<9K and Nb3Sn data for T>9K. The values of $H_{nuc}(0)$ and T_c are varied for each of the Nb and Nb3Sn data sets to yield the best fits to Equation 3. The resulting plots are presented in Fig. 7.

The best fit values of $H_{nuc}(0)$ and T_c for Nb and Nb3Sn are presented in Table 4. The values for Nb3Sn are close to the expected value of H_{c1} and T_c. The value for the Nb is higher than typical H_{c1} values and closer to values quoted for H_{sh}.

Table 3: Applied Entry Field and Vortex Nucleation Field as a Function of Temperature for the Coated Ellipsoid

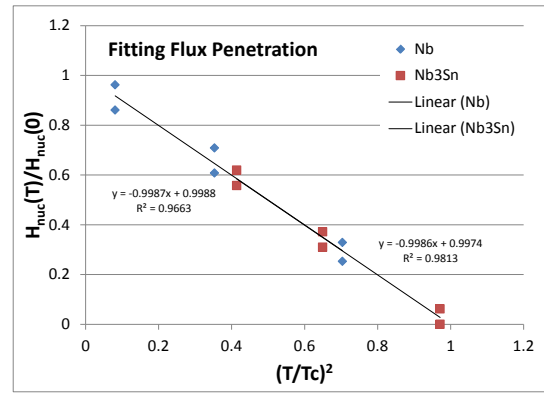| T [K]	$H_{applied\backslash entry}$(T) [mT]	$H_{nucleate}$(T) [mT]
2.66	180±10	207
5.56	130±10	149
7.85	57.5±7	66
11.1	19±1	21.8
13.9	11±1	12.6
17.0	1±1	1.15

Figure 7: Extracted data from flux penetration studies on the ellipsoid sample. Plotted are the estimated field of vortex nucleation as a function of temperature. Data with T<9K are normalized with H_{nuc} (0) and T_c of Nb and data with T>9K are normalized with H_{nuc} (0) and T_c of Nb3Sn. Best fits are given in Table 4.

Table 4: The Fitted H_{nuc}(0) and T_c for Nb and Nb3Sn Based on the Nb3Sn Coated Nb Ellipsoid Data

Material	$H_{nucleate}$ (0) [mT]	T_c [K]
Niobium	227	9.36
Nb3Sn	37.1	17.3

Coin Sample

The coin sample is tested in both transverse field and parallel field orientations as shown in Fig. 3a,b. The results of the tests for the parallel geometry are summarized in Fig. 8. For comparison a plot of the results for an uncoated Nb coin annealed at 1400C is also provided [2]. The Nb coin coated with Nb3Sn has an enhanced field of flux penetration compared to the annealed sample by about 20%.

The same data is normalized to T=0 using Equation 3 and to the estimated surface field based on the demagnetization analysis from Table 2. The results are plotted in Fig. 9. The results show that at $T=0$ the surface field would nucleate vortices at about 180mT for the annealed Nb disk while the field would nucleate vortices at 230mT for the coated Nb disk. The value from the annealed sample is near the expected value of H_{c1} for
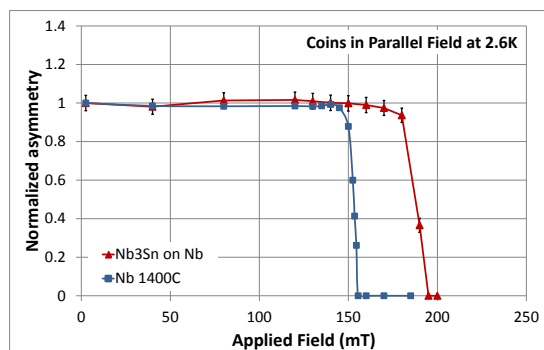

Figure 8: Normalized asymmetry as a function of applied field for coins in parallel field at 2.6K. The results compare a Nb sample annealed at 1400C and the Nb coin coated with Nb3Sn.
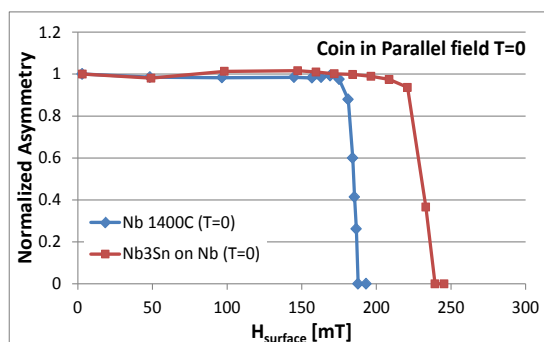
Figure 9: Same as Fig. 8 with the data normalized to the estimated surface field based on the demagnetization analysis from Table 2 and extrapolated to T=0 using Equation 3.

Nb. The nucleation field for the Nb3Sn on Nb coin replicates the findings for the ellipsoid geometry.

DISCUSSION

Recalling the discussion about geometry the estimate of the field of vortex nucleation based on the applied field assumes a pin free sample. To be confidant in the results an estimate of the level of pinning in the samples is required. Detailed explorations of the role of pinning are covered in another paper at the conference [2]. The analysis here will follow from those investigations. Since the Nb3Sn coating is applied at an elevated temperature (1100C) we expect, based on experience, that the pinning in the bulk is relatively small. To check this we compare the results from all three geometries at 2.6K. In order to make a direct comparison we normalize the applied fields with the geometric factors from Table 2 to get the surface fields and divide by $H_{nuc}(2.6K)$ from Table 4 and Equation 3. The results are plotted in Fig. 10.

Strong pinning manifests itself by delaying field penetration from the edges to the centre in the transverse coin set-up such that the normalized field for flux break in can be significantly higher than for the parallel geometry. Material with pinning is also characterized with an extended tail in the ellipsoid normalized field plot when compared to the parallel geometry normalized field plot. Fig. 10 indicates that neither characteristic of pinning is evident. In the transverse case flux breaks in primarily at $H_{nucleate}$. The tail in the transverse plot is typical of results from other annealed samples and does not indicate pinning. Some flux breaks in at low field. The source of this flux needs further investigation. In the ellipsoid case the flux breaks in at $H_{nucleate}$ with no tail. The plot indicates that pinning is quite weak in the coated samples so the results are not distorted by enhanced pinning.

The enhancement in $H_{nucleate}$ at T<9K for Nb coated with Nb3Sn is interesting. The Meissner state can persist metastably beyond H_{c1}, up to the superheating field H_{sh}, due to the Bean-Livingston surface energy barrier. However this barrier exists for magnetic fields parallel to a defect free surface. The ellipsoid provides a parallel surface at the equator where nucleation is expected and magnetization is uniform. However the high $H_{nucleate}$ value

is also replicated in the coin in parallel field result where the geometry is less favourable due to the sharp corners of the sample. It could be that Nb3Sn in mixed phase provides some channeling of the fluxoids near the Nb surface that helps promote a surface barrier. Tests with the coin geometry at 11K in the transverse geometry indicate some pinning and in the parallel geometry showed premature flux entry. Future tests are planned with coins in parallel/transverse fields at various temperatures to further investigate the augmentation in $H_{nucleate}$ for coated samples. The measurements of the Nb3Sn parameters are consistent with expectations in terms of both H_{c1} and T_c and not H_{sh}.
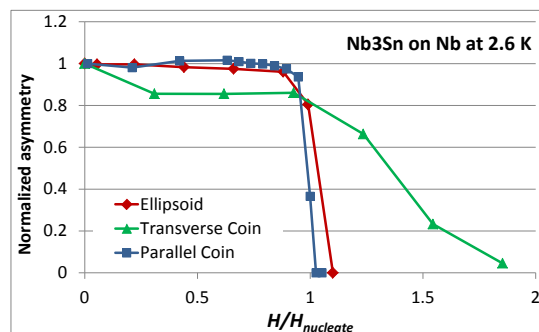

Figure 10: Results for all three geometries at 2.6K where applied fields are normalized with the geometric factors from Table 2 to get surface fields and then divided by the measured field strength required to nucleate vortices.

ACKNOWLEDGMENT

REFERENCES

[1] A. Grassellino, et al, 'Muon Spin Rotation Studies of Niobium for Superconducting RF Applications', Phys. Rev. ST Accel. Beams 16, 062002 (2013).

[2] R.E. Laxdal, et al, 'Characterization of SRF Materials at the TRIUMF μSR facility', Proc. SRF2015, http://jacow.org/.

[3] S. Posen, et al, 'Proof-of-principle demonstration of Nb3Sn superconducting radiofrequency cavities for high Q_0 applications', Appl. Phys. Lett. 106, 082601 (2015).

[4] A. Godeke, 'Nb3Sn for Radio Frequency Cavities', Report Number: LBNL-62140, (2006).

[5] M.K. Transtrum, et al, 'Superheating Field of Superconductors within Ginzburg-Landau Theory', Phys. Rev. B, 83(9):094505, March 2011.

[6] S. Gheidi, et al, 'First μSR Measurements of SRF Samples in Strong Parallel Fields', Proc. SRF2015, http://jacow.org/.

[7] S. Posen and M. Liepe, 'Advances in development of Nb3Sn superconducting radio-frequency cavities', Phys. Rev. ST Accel. Beams 15, 112001 (2014).

[8] E.H. Brandt, 'Superconductors in Realistic Geometries: geometric edge barrier vs pinning', Physica C 332 (2000) 99-107.